Title

After pruning, wind-induced bending moments and vibrations decrease more on reduced than raised Senegal mahogany (*Khaya senegalensis*)

Authors

Daniel C. Burcham[1,4]*, Wesley R. Autio[2], Yahya Modarres-Sadeghi[3], and Brian Kane[4]

[1]Centre for Urban Greenery and Ecology
National Parks Board
Singapore 259569

[2]Stockbridge School of Agriculture
University of Massachusetts Amherst
Amherst, MA 01003

[3]Department of Mechanical and Industrial Engineering
University of Massachusetts Amherst
Amherst, MA 01003

[4]Department of Environmental Conservation
University of Massachusetts Amherst
Amherst, MA 01003

*Corresponding author: danielburcham@gmail.com

Highlights

- Wind-tree interaction was examined before and after pruning large, open-grown trees
- Wind-induced vibration diminished as pruning severity increased on reduced trees
- After pruning, raised trees continued to vibrate at their fundamental mode
- At each pruning severity, wind loads decreased more on reduced than raised trees

Abstract (300 words)

Pruning is commonly used to mitigate the risk of tree failure by selectively removing tree parts exposed to the wind, but there have been few studies examining changes in wind loads after pruning, especially for large, open-grown trees. In this study, the wind-induced vibration and bending moments of Senegal mahogany (*Khaya senegalensis*) were monitored before and after a series of pruning treatments: crowns were either raised or reduced at incremental severities between 0 and 20%. Under ambient wind loads, axial trunk deformation was measured using two displacement probes installed orthogonally on each tree, and each displacement probe was calibrated using a static load test to convert the measured trunk deformation to a bending moment. During each pruning treatment, ambient wind conditions and trunk deformation were monitored simultaneously for extended periods of time. As pruning severity increased, Fourier spectra showed that raised trees continued to vibrate primarily at their fundamental mode, but reduced trees vibrated progressively less than raised trees. Similarly, the average 30-minute maximum bending moment, associated with a given 30-minute maximum wind speed, decreased more for reduced than raised trees. Consistent with existing studies of small trees, the results suggest that arborists should reduce trees to decrease wind loads and, concomitantly, the likelihood of tree failure. Still, excessive leaf loss may constrain the usefulness of increasingly severe pruning on reduced trees: average leaf area index decreased by half on trees reduced by 20%. More work is needed to understand the long-term physiological and mechanical consequences of pruning treatments.

Keywords

Biomechanics; Wind loads; Pruning; Wind-tree interaction

Introduction

Trees are often pruned to mitigate the risk of wind damage. Arborists attempt to reduce the likelihood of tree failure by selectively removing branches to improve crown structure, decrease leaf area, or increase crown porosity (Gilman and Lilly, 2019), but there is limited evidence available to inform the use of arboricultural pruning treatments for risk mitigation. Consistent with measurements of drag on unpruned trees (Kane et al., 2008; Rudnicki et al., 2004; Vollsinger et al., 2005), some studies reported that drag generally decreased after pruning in proportion to the mass of branches and foliage removed (Pavlis et al., 2008; Smiley and Kane, 2006). These results imply that drag can be minimized with increasingly severe pruning, but the adverse physiological consequences of excessive pruning, such as altered growth patterns (Fini et al., 2015), modified carbohydrate allocation (Haddad et al., 1995), or wood decay (Danescu et al., 2015), counteract the favorable decrease in wind loads. In most cases, arborists seek to manage risk without disproportionately limiting the physiological function and corresponding benefits of a tree (Song et al., 2018).

Arborists use different pruning techniques to achieve specific objectives (TCIA, 2017). Existing studies have shown that shortening branches to decrease tree height and crown spread, i.e., reduction pruning, most effectively decreased wind-induced bending moments (Pavlis et al., 2008; Smiley and Kane, 2006). Other studies reported inconsistent changes in tree movement associated with various pruning types (Gilman et al., 2008a, 2008b), but differences in experimental procedures likely caused some of the disparity between studies. Gilman et al. (2008a, 2008b) did not account for the variation in size among experimental trees during analysis, and trunk section properties have a large influence on tree deflection (Niklas, 1992). In most related work, the emphasis on measuring wind-induced bending moments near the lower trunk (Pavlis et al., 2008; Smiley and Kane, 2006) is understandable, since established measurement techniques exist for this quantity (Angelou et al., 2019; James and Kane, 2008) and the largest wind-induced forces occur in the lower trunk (Ennos, 2012).

Existing studies on the mechanical consequences of pruning were mostly limited to observations of small, young trees exposed to controlled wind conditions, such as those generated by wind tunnels (Rudnicki et al., 2004; Vollsinger et al., 2005), mechanical fans (Gilman et al., 2008a, 2008b), or moving trees through a weak or stationary wind field (Pavlis et al., 2008; Smiley and Kane, 2006). But experimentally regulated conditions are unlike the stochastic, dynamic wind environments commonly experienced by trees, and there are important mechanical differences between small and large trees (Anten et al., 2011) that prevent the application of existing results across a wide range of tree sizes. Although many have observed drag reduction by reconfiguration in small trees (Kane et al., 2008; Kane and Smiley, 2006; Rudnicki et al., 2004; Vollsinger et al., 2005), there is no evidence of similar behavior in large trees (Ennos, 1999), and it is unlikely that pruning will alter the aerodynamic properties of small and large trees equivalently (Rudnicki et al., 2004). Given concerns about public safety (Schmidlin, 2008) and legal liability (Mortimer and Kane, 2004) for tree failures, it is important to objectively inform the use of pruning treatments for risk mitigation, and this study was designed to determine the effect of arboricultural pruning treatments on the wind-induced movement and wind loads of large, open-grown tropical trees.

Methods

Site and trees

Data were collected from the same site and trees described in Burcham et al. (2020). Briefly, twelve Senegal mahoganies [*Khaya senegalensis* (Meliaceae)] were selected from a managed urban woodland near Choa Chu Kang, Singapore (latitude 1° 23’ N, longitude 103° 45’ E, elevation 10 m). The 5.5 ha even-aged stand contained 173 other large, mature *K. senegalensis* and rain tree [*Samanea saman* (Fabaceae)] (Figure 1) planted on an unknown date. The low planting density (~31 trees·ha^{-1}) allowed trees to develop an open-grown branch architecture mostly unaffected by competition from neighbors. Although the trees were not pruned during their growth and development, dead, damaged, and diseased branches were removed from experimental trees before the study. At the same time, the crowns of neighboring trees were selectively pruned to prevent collisions with experimental trees. Burcham et al. (2020) summarized the size and morphometric attributes of trees used in this study.

Instrumentation and signal processing

In the study, wind conditions and wind-induced tree movement were monitored simultaneously for extended time periods. Two LVDT displacement probes (Solartron Metrology, VS/20/U, West Sussex, UK) were used to measure axial deformation, $\boldsymbol{x}$ (mm), on the lower trunk of each tree. The probes measured up to 20 mm displacement over a linear distance of 226.9 mm with a measurement resolution of 10 μm and accuracy equivalent to 0.20% of output, yielding a strain resolution of 43 $\mu m \cdot m^{-1}$. Mounted on top of the bark using universal joints secured with hanger bolts, the probes were oriented axially (i.e., parallel to wood grain) and positioned on the North (0°) and East (90°) aspects of the trunk 1.37 m above the highest root.

To measure wind velocity, $\boldsymbol{u}$ ($m \cdot s^{-1}$), along a vertical gradient in the center of the experimental site (Figure 1), four ultrasonic anemometers (R.M. Young, Model 85106, Traverse City, MI, USA) were installed at 4.57 m intervals on an 18.3 m tall guyed mast (South Midlands Communications, PA2, Hampshire, England). The height, z (m), of anemometers normalized by the average height of experimental trees, H_{TREE} = 26.9 m, was 0.17, 0.34, 0.52, and 0.69. The anemometers measured wind speed within a range of 0 to 70 $m \cdot s^{-1}$ with a resolution of 0.1 $m \cdot s^{-1}$ and accuracy equivalent to 3% of output; and they recorded wind direction within a range of 0 to 360° with a resolution of 1° and ± 2° accuracy.

During the study, $\boldsymbol{u}$ and $\boldsymbol{x}$ were measured continuously at irregular intervals near 27 Hz, and 30-minute time histories of $\boldsymbol{u}$ and $\boldsymbol{x}$ were consistently used to examine wind-tree interactions over a range of time scales. For all recorded signals, missing values and those outside the measurement range of a given sensor were replaced using nearest neighbor linear interpolation. Subsequently, the mean was removed from each signal to obtain fluctuations about this value. Remaining spikes were identified as values greater than three standard deviations from a 1,000 sample moving mean and replaced with the nearest non-outlier value.

Wind-induced bending moments

To measure wind-induced bending moments, M_B (kN·m), static pull tests were used to determine a calibration constant, C_1 (MN), relating trunk deformation to an applied M_B for individual trees (Wellpott, 2008). Briefly, trees were pulled using a rope aligned incident to one of the displacement probes, and rope tension was measured with a digital dynamometer (EDXtreme-5T, Dillon, Fairmont, MN, USA) with 5,000 kg capacity, 1 kg resolution, and ± 5 kg accuracy. The incremental M_B generated at the height of measurement was calculated as:

$$M_B = F \cos\theta \, l, \qquad \text{Eq. 1}$$

where F is the force (N) applied by the rope; θ is the angle between the rope and a horizontal plane parallel to the ground; and l is the distance (m) between the rope attachment point and the midpoint of the displacement probe. C_1 was determined as the slope of an ordinary least-squares regression line fit to model M_B as a function of $\boldsymbol{x}$:

$$C_1 = M_B/\boldsymbol{x} \qquad \text{Eq. 2}$$

Rotation of the root-soil system was not monitored during pull testing. Burcham et al. (2020) provided more details about the tree pulling test methods.

Pruning treatments

Two pruning treatments commonly used in Singapore were examined in the study. Broadly according to ANSI A300 (Part 1) (TCIA, 2017), the crowns of experimental trees were either progressively raised by removing branches from the lower crown or reduced by shortening tree parts to decrease crown height. Pruning severity was determined as the percent change in crown length, L_{CROWN} (m), the vertical distance between the lowest branch and crown apex. For experimental consistency, the pruning treatments were applied using simple rules to cause similar changes to the crown dimensions of trees with different branch architecture. At each severity, branches were removed from a horizontal slice of the crown with a thickness equal to pruning severity multiplied by L_{CROWN}. For raised and reduced trees, the slices originated from the bottom and top of the crown, respectively. On reduced trees, all tree parts were removed from each horizontal slice, but only branches with a diameter less than 60% of its subtending member were removed from each horizontal slice on raised trees. Burcham et al. (2020) gave a detailed account of pruning treatments. Before pruning, wind conditions and wind-induced tree movement were monitored for 45 days, and each pruning treatment was similarly maintained for 45 days to record the same measurements.

Leaf condition

During the experiment, changes in leaf condition were examined by tracking leaf area index (LAI), an important variable controlling tree physiological processes (Running and Coughlan, 1988), over the sequence of pruning treatments. Initially, the relationship between leaf area and mass was determined by removing individual leaves from three *K. senegalensis* using multistage sampling. After dividing each crown into five vertical segments of equal length, fifteen leaf-bearing twigs were selected from different positions distributed throughout each segment, and all of the fully expanded leaves arranged around the three youngest leaf nodes on each twig were removed for measurement. The adaxial surface area, S_{LEAF} (m^2), and total fresh mass, m_{LEAF} (kg), of each leaf was measured using a leaf area meter (LI-3100C, LI-COR Biosciences, Lincoln, Nebraska, USA) and precision balance (EL-410S, Setra Systems, Inc., Boxborough, Massachusetts, USA), respectively. After measurement, the leaves were dried in a forced convection oven (Binder BIN-FD115, Tuttlingen, Germany) at 103° to practical equilibrium, and the dry mass of leaves was recorded using the same precision balance. The percent moisture content, MC (%), of leaves was determined as the percent change between fresh and dry mass. Using these measurements, the relationship between S_{LEAF} and m_{LEAF} was determined using ordinary least-squares regression.

At each pruning severity, the total fresh mass of leaves, m_{LEAF} (kg), removed from the tree was determined as the difference between the mass of pruned branches, measured with the EDXtreme-5T digital dynamometer, before and after removing leaves. After the final pruning treatment, the trees were felled to similarly determine the mass of the remaining leaves. Using these measurements, S_{LEAF} was estimated from m_{LEAF} using the empirical relationship fit to these two variables, and LAI was computed as the total single-sided area of leaves divided by the ground surface area occupied by the crown (Breda, 2003). At each pruning severity, the surface area occupied by the crown was estimated as the convex hull of the set of points determined by the outer extent of all primary branches projected onto the ground surface.

Spectral analysis

To examine the frequencies associated with wind-induced tree vibration, Fourier spectra were computed using selected 30-minute time histories of $\boldsymbol{x}$ at each pruning severity. After excluding 30-minute intervals coinciding with precipitation events, the variability in the direction of wind flow, χ (deg), was assessed using the unbiased estimate of the standard deviation of wind direction (Yamartino, 1984), and all intervals with $\sigma_\chi \geq 40°$ were excluded from further consideration. At each pruning severity, the set of qualifying 30-minute intervals was ranked according to mean wind speed, and the four intervals with the highest mean wind speeds were selected for spectral analysis.

Based on the assumption that drag primarily acts along the resultant wind vector, $\bar{\boldsymbol{u}}$ (Mayer, 1987; Schindler, 2008), scalar projections were made of $\boldsymbol{u}$ (wind velocity) and $\boldsymbol{x}$ (two-component trunk deformation) onto $\bar{\boldsymbol{u}}$ to obtain a scalar streamwise wind speed, u, and trunk deformation, x_u, and the Fourier energy spectrum, S(f), was computed using 30-minute time histories of x_u. Before analysis, time histories were down sampled to uniform 0.05 sec intervals (20 Hz) using nearest neighbor linear interpolation, and a 6th order infinite impulse response (IIR) Butterworth bandpass filter was used to remove long-term trends and short-term fluctuations associated with instrument noise.

The Fourier amplitude spectrum was computed for 16 sequential, non-overlapping segments of 2,048 observations using a Hanning window, and these spectra were ensemble averaged and smoothed to reduce artefacts (Konno and Ohmachi, 1998). Spectra were presented in semi-logarithmic format with f·S(f) plotted against 1,024 logarithmically spaced frequencies (Stull, 1988), since peaks are better associated with the correct scales using this transformation (Zangvil, 1981). Dominant frequencies associated with tree vibration were identified as those associated with the most prominent peaks in the computed Fourier spectra. All signal processing was performed in MATLAB (R2018b, MathWorks, Natick, MA, United States).

Experimental design and data analysis

The experiment was designed as a one-way repeated measures analysis of covariance (ANCOVA) with one between-subject factor with two levels (pruning type: raise, reduce) and one within-subject factor with three levels (pruning severity: 0, 10, 20%). During each experimental treatment, maximum wind-induced M_B and wind speed, U (m·s^{-1}), were selected from all available 30-minute intervals, and a covariate was used in the model to account for the relationship between 30-minute maximum M_B and 30-minute maximum U. Linear mixed effects models for repeated measures analysis of covariance were fit to 30-minute maximum M_B using proc mixed in SAS 9.4 (SAS Institute, Inc., Cary, NC, USA). Fixed effects for the model included pruning type, pruning severity, and their interaction. To minimize initial variability, trees were randomly assigned to pruning type after accounting for morphology, and the random effect of tree, nested within pruning type, was included in the model.

Using bivariate regression, the functional form of the covariate was determined by examining the relationship between 30-minute maximum M_B and 30-minute maximum U after a series of transformations provided by power, exponential, and logarithmic functions; and the mathematical form yielding the highest coefficient of determination in all cases was selected for consistent use. For all bivariate pairs, the validity of statistical assumptions for linear regression was checked, and the goodness of fit was tested using the F-test for lack of fit obtained from the regression ANOVA (Kutner et al., 2004). After determining the form of the covariate, the relationship between 30-minute maximum M_B and 30-minute maximum U was examined separately for wind measurements from different anemometers, and the anemometer with measurements yielding the highest coefficient of determination was used consistently for the analysis of wind-induced M_B.

Model variance-covariance matrix structures were examined using information criteria, and the covariance structure with the algebraically minimal Bayesian Information Criterion (BIC), a common model selection index, was selected. The Kenward-Roger correction was used to adjust the error degrees of freedom for the selected covariance structure. Subsequently, the homogeneity of slopes among fixed effects was tested and, if rejected, an unequal slopes model was fit to observations. Fixed effects were tested with the covariate set equal to 5 $m \cdot s^{-1}$. For significant fixed effects, least squares (LS) means were computed at three values of the covariate distributed over the upper range of observed 30-minute maximum wind speeds. Significant interactions were separated to determine the effect of pruning severity within each pruning type. Regression was used to separate means associated with specific levels of pruning severity. Single-degree-of-freedom orthogonal polynomial comparisons (OPC) were made to assess the significance of individual polynomial terms, and least squares regression was used to determine the associated polynomial coefficients. An *F*-test was used to evaluate the mean difference between pruning types at 0% severity (i.e., before pruning).

Results

Wind conditions

Although differences existed among experimental periods, wind conditions were generally calm during the entire experiment. Among all 30-minute intervals (n = 3,623), approximately 12% of 30-minute mean wind speeds measured at z/H_{TREE} = 0.69 exceeded 1 $m \cdot s^{-1}$. The maximum 30-minute mean and instantaneous wind speed measured at the same height was 2.0 $m \cdot s^{-1}$ and 7.3 $m \cdot s^{-1}$, respectively. During the entire experiment, the modal prevailing 30-minute direction of wind flow was south (S).

Mean wind speeds increased slightly over the course of the experiment (Figure 2). During the first 45 days of the experiment before trees were pruned, wind speeds and directions were relatively low and variable, respectively. Among all 30-minute intervals, the resultant direction of wind flow was mostly distributed between south-southeast (SSE) and northwest (NW), although most of the highest wind speeds were recorded in wind flow moving towards the east (E). During the 45-day period after trees were pruned 10%, the mean winds increased slightly and blew more consistently towards SSE compared to the preceding 45-day period. Although the resultant direction of wind flow was increasingly concentrated towards SSE, some of the highest wind speeds were recorded in wind flow moving towards S. During the 45-day period after trees were pruned 20%, mean winds increased considerably compared to the preceding experimental periods and blew near consistently towards S, with one-third of all observations occurring between 185° and 195°.

Leaf condition

For the sampled leaves, there was a significant (F = 2667.3; df = 1, 279; p < 0.001) linear relationship between S_{LEAF} and m_{LEAF} (Figure 3). Expressed in relation to dry mass, the average percent moisture content of all measured leaves was 119% (SD 14). Among unpruned trees, LAI was initially similar, on average, for trees designated to be raised (mean: 8.7; SD: 5.1) and reduced (mean: 8.2; SD: 2.6), but there was a noticeable difference in the post-pruning trends in average LAI for raised and reduced trees. After pruning, LAI increased slightly, on average, for trees raised by 10% (mean: 9.4; SD: 5.0) and 20% (mean: 9.2; SD: 4.6). For these trees, the projected crown area declined slightly faster than total leaf area. In contrast, LAI decreased considerably, on average, for trees reduced by 10% (mean: 6.7; SD: 1.5) and 20% (mean: 4.1; SD: 1.1) because total leaf area declined much faster than the projected crown area for these trees.

Fourier spectra

One tree was removed from the study following unintentional root damage during free vibration testing for a separate experiment, and the total number of reduced trees decreased by one to five. Due to instrument failures, measurements of all trees were not consistently available for spectral analysis, but all available data in each selected 30-minute interval were used to analyze measurements for as many trees as possible (Table 1). Before pruning, Fourier energy spectra computed from 30-minute time histories of x_u showed prominent peaks between 0.11 and 0.25 Hz (mean: 0.16 Hz) (Figure 4A – D). In most cases, there was a single characteristic peak in Fourier energy, indicating that trees mostly vibrated in a narrow range of frequencies during these wind events. During a given wind event, Fourier energy associated with the most prominent peak varied among all trees, reflecting differences in the amplitude of trunk vibration at this frequency over the entire 30-minute interval. For several trees, there was a second, less prominent peak at lower frequencies between 0.02 and 0.04 Hz. During these wind events, unpruned trees assigned to the reduced treatment group often experienced greater wind excitation at all frequencies, including the most prominent frequency, than trees assigned to the raised treatment group. On average, total Fourier energy was 14% greater for unpruned trees designated to be reduced than others to be raised, and Fourier energy associated with the most prominent peak was, on average, 13% greater for the former than latter before pruning.

For trees raised by 10%, prominent peaks in Fourier energy existed at frequencies similar to those observed before pruning (Figure 4E – H). By comparison, less prominent peaks existed at slightly higher frequencies for trees reduced by the same amount, despite a broad concentration of Fourier energy in the range of analyzed frequencies. Spectral estimates showed that the dominant frequency of wind-induced trunk vibration for trees raised and reduced by 10%, respectively, was similar to (mean: 0.16 Hz; range: 0.13 – 0.23 Hz) and greater than (mean: 0.19 Hz; range: 0.13 – 0.25 Hz) those observed before pruning. For reduced trees, Fourier energy associated with the most prominent peak was, on average, 10% less than raised trees, indicating that reduced trees mostly vibrated at slightly higher frequencies with a smaller amplitude during these wind events. On average, total Fourier energy for reduced trees was 1% less than raised trees, reflecting a smaller amplitude of vibration across all analyzed frequencies.

For trees reduced by 20%, there were no obvious, prominent peaks in Fourier energy computed from 30-minute x_u time histories, especially compared to the energy spectra associated with trees raised by 20% (Figure 4I – L). Fourier energy spectra computed from 30-minute x_u time histories of trees raised by 20% mostly showed peak frequencies (mean: 0.17 Hz; range: 0.12 – 0.23 Hz) similar to those observed during wind-induced vibration in preceding experimental periods. For a given wind event, variability in power associated with the most prominent peak among raised trees was commensurate with other experimental periods and indicated uneven wind-induced excitation of these trees during each 30-minute interval. On average, total Fourier energy was 63% less for reduced than raised trees, indicating a considerable decrease in wind-induced vibration for reduced trees at all analyzed frequencies.

Wind-induced bending moments

Arising from differences in tree stiffness, the measurement resolution of wind-induced M_B varied according to C_1 for each tree between 6 and 18.5 kN·m. For the entire experiment, wind-induced M_B varied between 0 and 278 kN·m, reflecting the relatively mild wind conditions encountered at the site. At 0% severity, visual inspection of scatter plots revealed a curvilinear relationship between 30-minute maximum M_B and 30-minute maximum U. In broad agreement with theory, a positive quadratic function best described the relationship between these two variables for individual unpruned trees, and the greatest proportion of variance in 30-minute maximum M_B was accounted for by 30-minute maximum U measured on the anemometer positioned closest to the canopy apex at z/H_{TREE} = 0.69 (Figure 5). As a result, only wind measurements recorded by this anemometer positioned nearest to the canopy apex were used to analyze wind-induced M_B.

Although the relationship between 30-minute maximum M_B and 30-minute maximum U was quadratic for all trees at 0% severity, visual inspection of scatter plots indicated that the form of this relationship was affected by pruning severity, especially on reduced trees. Scatter plots of 30-minute maximum M_B and 30-minute maximum U showed different patterns for individual raised and reduced trees at 10% and 20% severity. A second-order polynomial with a positive quadratic term best described the relationship between these two variables for individual raised trees at all severities, but the quadratic term approached zero and became negative at 10% and 20%, respectively, for most reduced trees (Figure 6). Scatter plots of 30-minute maximum M_B and 30-minute maximum U for individual trees showed similar trends (Online Resource 1).

In total, 12,455 observations of 30-minute maximum M_B and 30-minute maximum U were obtained from 3,623 separate 30-minute intervals between 0 and 20% pruning severity. Only four covariance structures with limited parameters were examined, since it was computationally expensive to fit covariance structures with a large number of parameters to this dataset. Among these, the BIC fit index indicated that first-order autoregressive moving average [ARMA(1,1)] best fit the 30-minute maximum M_B dataset.

As expected, there was a highly significant linear relationship between 30-minute maximum M_B and 30-minute maximum U^2 (F = 407; df = 6, 8539; p < 0.001), and the slopes describing 30-minute maximum M_B as a function of 30-minute maximum U^2 varied significantly among combinations of pruning type and severity (F = 78.7; df = 2, 8600; p < 0.001). As a result, unequal slopes were fit to describe the relationship between 30-minute maximum M_B and U^2 for each combination of pruning type and severity separately (Table 2). For raised trees, the slopes fit to describe 30-minute maximum M_B as a function of 30-minute maximum U^2 decreased by 9% and 30%, respectively, at 10% and 20% severity relative to the same at 0% severity, reflecting a moderate decrease in the maximum wind-induced M_B across all observed wind speeds. For reduced trees, these slopes decreased by 46% and 94%, respectively, at 10% and 20% severity, reflecting a substantial decrease in the maximum wind-induced M_B across all measured wind speeds.

Statistical inferences about fixed effects were made with the covariate set equal to 5 $m \cdot s^{-1}$ (U^2 = 25 $m \cdot s^{-1}$), a value near the upper limit of observed wind speeds (Table 3). For trees exposed to a 30-minute maximum wind speed of 5 $m \cdot s^{-1}$, analysis of covariance indicated that the average 30-minute maximum M_B did not vary significantly between pruning types, but the average 30-minute maximum M_B varied significantly among pruning severities, reflecting a decrease in wind loads with increasing severity of pruning. However, pruning type and severity interacted significantly to affect the average 30-minute maximum M_B of trees exposed to a 30-minute maximum wind speed of 5 $m \cdot s^{-1}$. Although the average 30-minute maximum M_B decreased significantly with the severity of pruning for both raised and reduced trees, there was a greater decrease in the average 30-minute maximum M_B on reduced than raised trees across all severities.

Mean separation was performed at three wind speeds chosen to represent the upper range of 30-minute maximum U observed in this study: 4, 5, and 6 $m \cdot s^{-1}$ (Figure 7). For raised trees, OPC revealed a quadratic decrease in the average 30-minute maximum M_B with pruning severity for all wind speeds, reflecting a negligible and moderate decrease, respectively, in the average 30-minute maximum M_B at 10% and 20% severity. For reduced trees, OPC revealed a linear decrease in the average 30-minute maximum M_B with pruning severity for all wind speeds, reflecting a continuous decrease in the maximum wind-induced M_B across all severities. Overall, means showed that the magnitude of 30-minute maximum M_B on raised trees decreased moderately at 20% severity, but the 30-minute maximum M_B continued to vary in proportion to 30-minute maximum U across all severities on these trees. In contrast, the magnitude of wind loads on reduced trees decreased considerably at both 10% and 20% severity, and the proportionality between 30-minute maximum M_B and 30-minute maximum U diminished with pruning severity on these trees, reflecting a more pronounced change in wind-tree interaction on reduced trees. Combining these results with mass measurements for the same trees (Burcham et al., 2020), the average decrease in 30-minute maximum M_B associated with a 30-minute maximum wind speed of 6 $m \cdot s^{-1}$, per unit mass removed, for trees raised and reduced by 10% was 5.8 and 38.8 $N \cdot m \cdot kg^{-1}$, respectively; and the same decrease for trees raised and reduced by 20% was 19.2 and 33.6 $N \cdot m \cdot kg^{-1}$, respectively.

Discussion

The low wind speeds observed in this study were consistent with meteorological observations in Singapore (Micheline and Ng, 2012) and similar studies of wind-tree interaction in other climates (Schindler, 2008; Schindler et al., 2013b). In future work, it will be important to study the effect of pruning treatments on trees experiencing higher wind speeds, since observations were constrained to mild, non-destructive wind loads in this study. Still, the wind conditions in this study inherently reflected the stochastic, dynamic wind loads commonly experienced by trees, and the results provide a valuable comparison with existing similar work on small trees in controlled wind flow.

Before pruning, the most prominent frequency of vibration during wind events closely matched the fundamental frequency of the same trees measured in free vibration (Burcham et al., 2020), and the predominant vibration of trees near their fundamental frequency during wind-induced motion is consistent with existing reports (Schindler et al., 2010; Sellier et al., 2008). Although the magnitude of peaks in Fourier energy was not consistent among spectra computed for all trees in a given wind event, it was expected that variability in the exposure of trees to a heterogenous wind field contributed to differences in excitation. In forest landscapes, many reports have demonstrated that trees are mostly excited by gusts arising from organized turbulence occurring at frequencies below their fundamental mode (Gardiner, 1995; Schindler et al., 2013a; Schindler and Mohr, 2019), and the secondary peaks occasionally observed in Fourier spectra were likely associated with the momentum transferred by such coherent structures at lower frequencies (Schindler et al., 2013a).

The lack of an obvious change in the frequency of raised trees at any pruning severity aligned with free vibration tests of the same trees (Burcham et al., 2020), indicating that raised trees continued to dissipate wind energy by swaying at their fundamental mode. But this was not true for reduced trees, for which the amplitude of vibration was progressively less than raised trees at each severity. Although some prominent peaks at higher frequencies were evident in Fourier spectra for trees reduced by 10%, wind loads acting on reduced trees were increasingly insufficient, as pruning severity increased, to cause the trunk deflection needed to induce vibration near the fundamental mode. For reduced trees, some of the residual power in the range of analyzed frequencies at higher severities was likely caused by instrument noise.

The use of period maxima to characterize wind-induced M_B on trees was consistent with existing work (Jackson et al., 2019; Wellpott, 2008). Although material fatigue caused by cyclical loading over time may precede tree failure in some cases (Rodgers et al., 1995), most authors assume that extreme (maximum) wind loads are the most frequent cause of failures (Gardiner et al., 2008). Schindler et al. (2016) showed that maximum gust speeds were the most important predictor of storm damage caused by a winter storm in southwest Germany, and other authors have similarly assumed that natural disturbances are driven by extreme value processes (Denny and Gaines, 1990).

Although the observed quadratic relationship between 30-minute maxim M_B and 30-minute maximum U agreed with theory (de Langre, 2008) and existing experimental observations (Hale et al., 2012), the functions explained less variance in 30-minute maximum M_B than reported in previous studies (Hale et al., 2012; Wellpott, 2008). In this study, the increased variability could be explained by the physical separation between anemometers and trees or the restriction of wind measurements to the turbulent canopy layer (Raupach et al., 1996). In addition to U (Flesch and Wilson, 1999; Peltola, 1996), existing studies showed that Reynold's stress (Mayer, 1987) or momentum flux (Schindler and Mohr, 2018) measured near the canopy apex best explained tree movement, but it was not possible to compute these higher-order statistics in this study using two-dimensional wind measurements. In the future, authors should measure three-dimensional wind flow near the crown apex and, as far as possible, ensure close proximity between wind flow and tree measurements.

In this study, the relatively low strain resolution of displacement probes (James and Kane 2008) and mild wind conditions resulted in the sensors operating near their limits of detection and contributed additional, unknown variability to observations. The low strain resolution of displacement probes caused similarly coarse M_B measurements. In terms of C_1, James (2010) measured M_B in much smaller increments, between 0.01 and 1.13 kN·m, than possible in this study. In the future, authors should carefully consider measurement resolution in light of anticipated wind loading conditions. Still, the estimation of maximum M_B should be less affected than mean M_B by this limitation (Gardiner, 1995).

The covariates fit to describe 30-minute maximum M_B as a function of 30-minute maximum U for each treatment combination showed that wind-tree interaction was more drastically altered on reduced than raised trees. Although both pruning types decreased the size of the crown exposed to the wind, the length of tree parts was simultaneously shortened on reduced trees, and this distinction likely explains the observed difference in wind loads between the two pruning types. Although several studies demonstrated that drag is proportional to mass (Rudnicki et al., 2004; Vollsinger et al., 2005), others have shown a greater decrease in wind-induced M_B, per unit decrease in mass, on reduced than raised trees (Pavlis et al., 2008). Leaves contribute significantly to total drag (Vollsinger et al., 2005), and they were removed faster on reduced than raised trees because leaves were concentrated near the canopy apex on these trees (Burcham et al., 2020). Reduced tree parts were also less exposed to faster-moving air at higher positions, since wind speed increases non-linearly above the ground in forests (Raupach et al., 1996). In addition, the average height at which drag acted, corresponding to the center of pressure height, was lowered on reduced trees, shortening the distance over which drag causes M_B on reduced trees (Pavlis et al., 2008).

Broadly, these observations agree with existing reports that M_B decreased more on reduced than raised trees (Pavlis et al., 2008; Smiley and Kane, 2006), and the consistency of findings for small and large trees gives assurance to arborists contemplating the use of pruning as a risk mitigation strategy. Since M_B decreased more, per unit mass removed, on reduced than raised trees, less mass needs to be removed from a reduced tree to cause a unit decrease in wind-induced M_B. Although this study did not examine all pruning methods tested in other studies, most existing reports consistently showed that M_B decreased most, at a given severity, on reduced trees compared to others pruned differently (Pavlis et al., 2008; Smiley and Kane, 2006). However, the marginal benefit of increasingly severe pruning for reduced trees should be carefully examined in future studies, especially since wind loads will change as trees grow after pruning.

Although this study acknowledges that trees are often pruned to reduce risk, it is equally important to consider the long-term implications of pruning on tree growth and vitality. In this study, LAI decreased by half, on average, for trees reduced by 20%, and this reveals an additional constraint to minimizing the risks presented by trees in constructed landscapes. For reduced trees, the physiological impairments from leaf loss may offset any favorable decrease in wind loads after pruning, and the implications of severe leaf loss should be examined in future work. Practical experience suggests that excessive pruning is unnecessary and possibly detrimental to trees – professional standards discourage removing more branches and leaves than necessary to meet pruning objectives (TCIA, 2017). Severe defoliation can alter resource allocation patterns and diminish stored carbohydrates available for future growth and defense (Landhausser and Lieffers, 2012), and most studies show that removing small branches with properly-executed pruning cuts will minimize similar issues (Fini et al., 2015; Ramirez et al., 2018). Topping, the practice of arbitrarily shortening tree parts without considering tree anatomy, removes apical control to favor the production of neoformed sprouts at the expense of secondary growth (Fini et al., 2015), and there is compelling evidence against the indiscriminate use of heading cuts during topping (Grabosky and Gilman, 2007). More work is needed to understand the long-term biological and mechanical consequences of pruning treatments.

Conclusion

In this study, wind loads decreased more on reduced than raised *K. senegalensis* because the two pruning types altered the size and location of tree parts differently. Assuming no change in the load-bearing capacity of the remaining tree parts, these results indicate that the likelihood of failure will decrease more for reduced than raised trees at a given severity of pruning, in proportion to the decrease in loads acting on these trees. In practice, trees are often pruned to meet specific objectives, and there are usually multiple reasons for pruning a tree in a landscape. If tree risk mitigation is a reason for pruning, these results suggest that arborists should reduce the size of the crown by shortening the length of tree parts, but this should be done carefully to avoid unnecessary changes, since a modest decrease in tree height caused a significant decrease in wind loads.

Acknowledgments

This work was supported by the National Parks Board, Singapore.

Literature Cited

Angelou, N., Dellwik, E., Mann, J., 2019. Wind load estimation on an open-grown European oak tree. Forestry 1–12. https://doi.org/10.1093/forestry/cpz026

Anten, N.P.R., Barton, K.E., Boege, K., Bond, B.J., Bond-Lamberty, B., Bucci, S.J., Cermak, J., Dawson, T.E., Day, M.E., Dickman, L.T., Dirzo, R., Evans, R., Ewers, B.E., Fouts, W., Goldstein, G., Greenwood, M.S., Hinckley, T.M., Hoch, G., Holtta, T., Ishii, H., Johnson, D.M., King, D.A., Lachenbruch, B., Mackay, D.S., McCulloh, K.A., McDowell, N.G., Meinzer, F.C., Mencuccini, M., Moore, J.R., Nadezhdina, N., Niinemets, U., Phillips, N.G., Reinhardt, K., Ryan, M.G., Sala, A., Scholz, F.G., Selaya, N.G., Steppe, K., Teskey, R.O., Thomas, S.C., Voelker, S.L., Whitehead, D., Woodruff, D.R., 2011. Size- and Age-Related Changes to Tree Structure and Function. Springer, Dordrecht, The Netherlands.

Breda, N.J.J., 2003. Ground-based measurements of leaf area index: A review of methods, instruments, and current controversies. J. Exp. Bot. 54, 2403–2417.

Burcham, D.C., Autio, W.R., James, K., Modarres-Sadeghi, Y., Kane, B., 2020. Effect of pruning type and severity on vibration properties and mass of Senegal mahogany (*Khaya senegalensis*) and rain tree (*Samanea saman*). Trees 34, 213–228. https://doi.org/10.1007/s00468-019-01912-8

Danescu, A., Ehring, A., Bauhus, J., Albrecht, A., Hein, S., 2015. Modelling discoloration and duration of branch occlusion following green pruning in *Acer pseudoplatanus* and *Fraxinus excelsior*. For. Ecol. Manage. 335, 87–98.

de Langre, E., 2008. Effects of wind on plants. Annu. Rev. Fluid Mech. 40, 141–168.

Denny, M.W., Gaines, S.D., 1990. On the prediction of maximal intertidal wave forces. Limnol. Oceanogr. 35, 1–15.

Ennos, A.R., 2012. Solid Biomechanics, 1st ed. Princeton University Press, Princeton, NJ, USA.

Ennos, A.R., 1999. The aerodynamics and hydrodynamics of plants. J. Exp. Bot. 292, 3281–3284.

Fini, A., Frangi, P., Faoro, M., Piatti, R., Amoroso, G., Ferrini, F., 2015. Effects of different pruning methods on an urban tree species: A four-year-experiment scaling down from the whole tree to the chloroplasts. Urban For. Urban Greening 14, 664–674.

Flesch, T.K., Wilson, J.D., 1999. Wind and remnant tree sway in forest cutblocks. II. Relating measured tree sway to wind statistics. Agric. For. Meteorol. 93, 243–258.

Gardiner, B.A., 1995. The interactions of wind and tree movement in forest canopies, in: Coutts, M.P., Grace, J. (Eds.), Wind and Trees. University of Cambridge, Cambridge, UK, pp. 41–59.

Gardiner, B.A., Byrne, K., Hale, S., Kamimura, K., Mitchell, S.J., Peltola, H., Ruel, J.C., 2008. A review of mechanistic modelling of wind damage risk to forests. Forestry 81, 447–463.

Gilman, E.F., Grabosky, J.C., Jones, S., Harchick, C., 2008a. Effects of pruning dose and type on trunk movement in tropical storm winds. Arboric. Urban For. 34, 13–19.

Gilman, E.F., Lilly, S.J., 2019. Tree Pruning, 3rd ed. International Society of Arboriculture, Champaign, Illinois.

Gilman, E.F., Masters, F., Grabosky, J.C., 2008b. Pruning affects tree movement in hurricane force wind. Arboric. Urban For. 34, 20–28.

Grabosky, J.C., Gilman, E.F., 2007. Response of two oak species to reduction pruning cuts. Arboric. Urban For. 33, 360–366.

Haddad, Y., Clair-MacZulajtys, D., Bory, G., 1995. Effects of curtain-like pruning on distribution and seasonal patterns of carbohydrate reserves in plane (*Platanus ×acerifolia* Wild) trees. Tree Physiol. 15, 135–140.

Hale, S.E., Gardiner, B.A., Wellpott, A., Nicoll, B.C., Achim, A., 2012. Wind loading of trees: Influence of tree size and competition. Eur. J. For. Res. 131, 203–217.

Jackson, T., Shenkin, A., Wellpott, A., Calders, K., Origo, N., Disney, M., Burt, A., Raumonen, P., Gardiner, B.A., Herold, M., Fourcaud, T., Malhi, Y., 2019. Finite element analysis of trees in the wind based on terrestrial laser scanning data. Agric. For. Meteorol. 265, 137–144.

James, K.R., 2010. A dynamic structural analysis of trees subjected to wind loading (PhD Thesis).

James, K.R., Kane, B., 2008. Precision digital instruments to measure dynamic wind loads on trees during storms. Agric. For. Meteorol. 148, 1055–1061.

Kane, B., Pavlis, M., Harris, J.R., Seiler, J.R., 2008. Crown reconfiguration and trunk stress in deciduous trees. Can. J. For. Res. 38, 1275–1289.

Kane, B., Smiley, E.T., 2006. Drag coefficients and crown area estimation of red maple. Can. J. For. Res. 36, 1951–1958.

Konno, K., Ohmachi, T., 1998. Ground-motion characteristics estimated from spectral ratio between horizontal and vertical components of microtremor. Bull. Seismol. Soc. Am. 88, 228–241.

Kutner, M.H., Nachtsheim, C.J., Neter, J., 2004. Applied Linear Regression Models, 4th ed. McGraw-Hill Irwin, Boston, MA, USA.

Landhausser, S.M., Lieffers, V.J., 2012. Defoliation increases risk of carbon starvation in root systems of mature aspen. Trees 26, 653–661.

Mayer, H., 1987. Wind-induced tree sways. Trees 1, 195–206.

Micheline, F., Ng, L.K., 2012. The Weather and Climate of Singapore. Meteorological Service Singapore, National Environment Agency, Singapore.

Mortimer, M.J., Kane, B., 2004. Hazard tree liability in the United States: Uncertain risks for owners and professionals. Urban For. Urban Greening 2, 159–165.

Niklas, K.J., 1992. Plant Biomechanics: An Engineering Approach to Plant Form and Function, 1st ed. University of Chicago Press, Chicago, IL, USA.

Pavlis, M., Kane, B., Harris, J.R., Seiler, J.R., 2008. The effects of pruning on drag and bending moment of shade trees. Arboric. Urban For. 34, 207–215.

Peltola, H., 1996. Swaying of trees in response to wind and thinning in a stand of Scots pine. Boundary Layer Meteorol. 77, 285–304.

Ramirez, J.A., Handa, I.T., Posada, J.M., Delagrange, S., Messier, C., 2018. Carbohydrate dynamics in roots, stems, and branches after maintenance pruning in two common urban tree species of North America. Urban For. Urban Greening 30, 24–31.

Raupach, M.R., Finnigan, J.J., Brunet, Y., 1996. Coherent eddies and turbulence in vegetation canopies: The mixing layer analogy. Boundary Layer Meteorol. 78, 351–382. https://doi.org/10.1007/BF00120941

Rodgers, M., Casey, A., McMenamin, C., Hendrick, E., 1995. An experimental investigation of the effects of dynamic loading on coniferous trees planted on wet mineral soils, in: Coutts, M.P., Grace, J. (Eds.), Wind and Trees. Cambridge University Press, New York, NY, USA, pp. 204–219.

Rudnicki, M., Mitchell, S.J., Novak, M.D., 2004. Wind tunnel measurements of crown streamlining and drag relationships for three conifer species. Can. J. For. Res. 34, 666–676.

Running, S.W., Coughlan, J.C., 1988. A general model of forest ecosystem processes for regional applications I. Hydrological balance, canopy gas exchange, and primary production processes. Ecol. Modell. 42, 125–154.

Schindler, D., 2008. Responses of Scots pine trees to dynamic wind loading. Agric. For. Meteorol. 148, 1733–1742.

Schindler, D., Fugmann, H., Mayer, H., 2013a. Analysis and simulation of dynamic response behavior of Scots pine trees to wind loading. Int. J. Biometeorol. 57, 819–833.

Schindler, D., Jung, C., Buchholz, A., 2016. Using highly resolved maximum gust speed as predictor for forest storm damage caused by the high-impact winter storm Lothar in Southwest Germany. Atmos. Sci. Lett. 17, 462–469.

Schindler, D., Mohr, M., 2019. No resonant response of Scots pine trees to wind excitation. Agric. For. Meteorol. 265, 227–244.

Schindler, D., Mohr, M., 2018. Non-oscillatory response to wind loading dominates movement of Scots pine trees. Agric. For. Meteorol. 250–251, 209–216.

Schindler, D., Schonborn, J., Fugmann, H., Mayer, H., 2013b. Responses of an individual deciduous broadleaved tree to wind excitation. Agric. For. Meteorol. 177, 69–82.

Schindler, D., Vogt, R., Fugmann, H., Rodriguez, M., Schonborn, J., Mayer, H., 2010. Vibration behavior of plantation-grown Scots pine trees in response to wind excitation. Agric. For. Meteorol. 150, 984–993.

Schmidlin, T.W., 2008. Human fatalities from wind-related tree failures in the United States, 1995-2007. Nat. Hazards 50, 13–25.

Sellier, D., Brunet, Y., Fourcaud, T., 2008. A numerical model of tree aerodynamic response to a turbulent airflow. Forestry 81, 279–297.

Smiley, E.T., Kane, B., 2006. The effects of pruning type on wind loading of *Acer rubrum*. Arboric. Urban For. 32, 33–40.

Song, X.P., Tan, P.Y., Edwards, P., Richards, D., 2018. The economic benefits and costs of trees in urban forest stewardship: A systematic review. Urban For. Urban Greening 29, 162–170.

Stull, R.B., 1988. An Introduction to Boundary Layer Meteorology. Kluwer Academic Publishing, Boston, MA.

TCIA, 2017. American National Standard for Tree Care Operations - Tree, Shrub, and Other Woody Plant Management - Standard Practices (Pruning). Tree Care Industry Association, Inc, Londonderry, NH, USA.
Vollsinger, S., Mitchell, S.J., Byrne, K.E., Novak, M.D., Rudnicki, M., 2005. Wind tunnel measurements of crown streamlining and drag relationships for several hardwood species. Can. J. For. Res. 35, 1238–1249.
Wellpott, A., 2008. The stability of continuous cover forests (PhD Thesis).
Yamartino, R.J., 1984. A comparison of several “single-pass” estimators of the standard deviation of wind direction. J. Clim. Appl. Meteorol. 23, 1362–1366.
Zangvil, A., 1981. Some aspects of the interpretation of spectra in meteorology. Boundary Layer Meteorol. 21, 39–46.

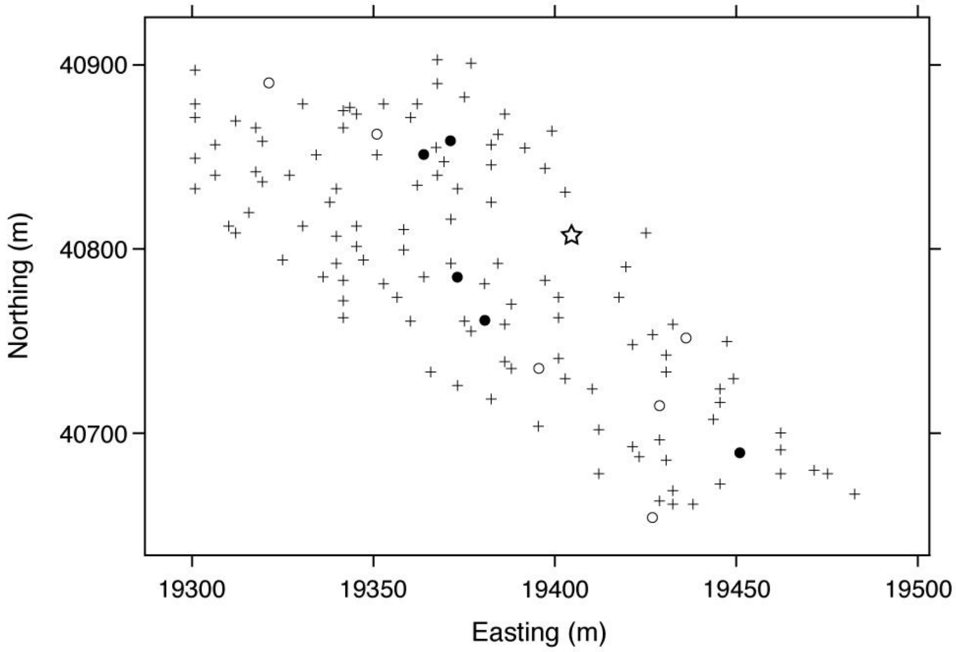

Figure 1: Site plan showing the location of experimental Senegal mahoganies (*Khaya senegalensis*, circle marker) among other trees not involved in the study (plus marker) and the guyed mast supporting anemometers (star marker). Raised and reduced trees are identified using empty and filled symbols, respectively. Northing and easting units (m) represent distance from an artificial origin at 103° 50’ 00’’ E, 1° 22’ 00’’ N.

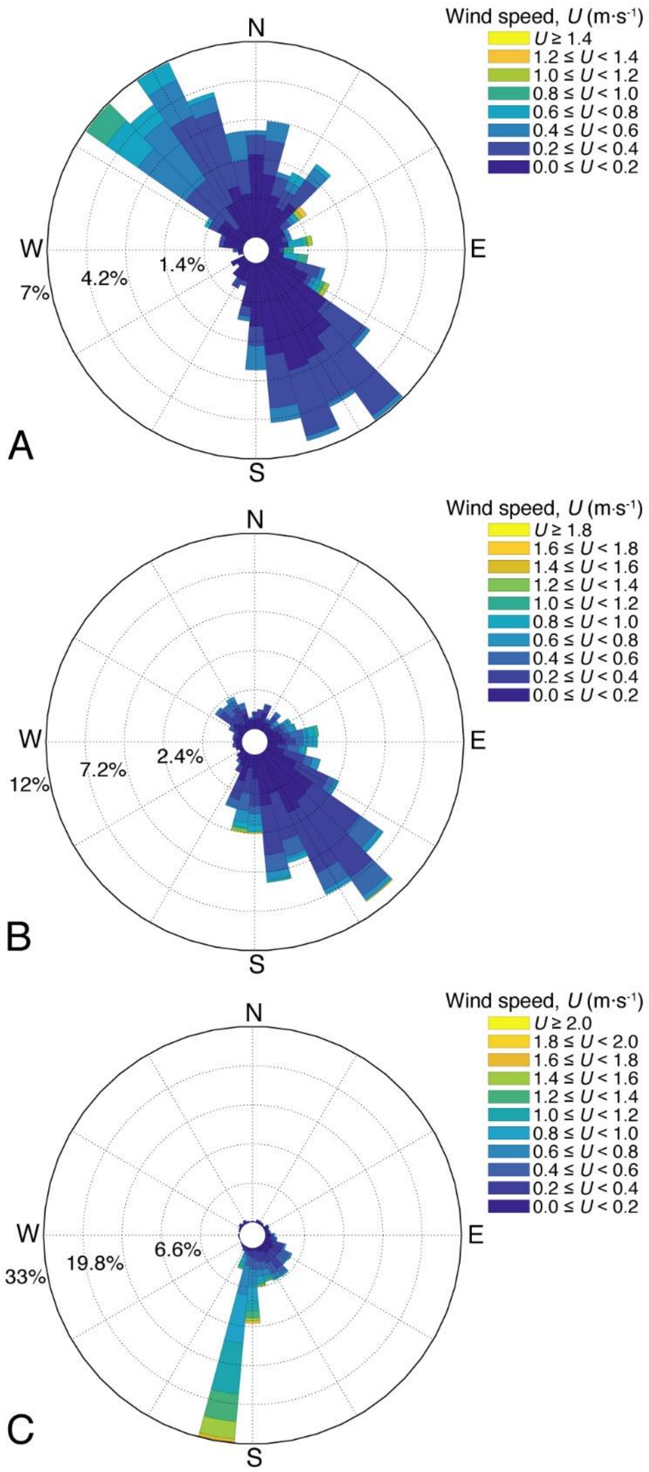

Figure 2: For 0% (A), 10% (B), and 20% (C) pruning severities, wind rose showing the relative frequency of 30-minute resultant wind speeds and directions for all available 30-minute intervals at the experimental site (n = 3,623). For measurements at 18.3 m (z/H_{TREE} = 0.69), the length of spokes depicts the relative frequency of 30-minute resultant wind directions, within 36 incremental 10° bins, for a given wind speed range denoted by color bands. Concentric circles are labeled to show the relative frequency of winds.

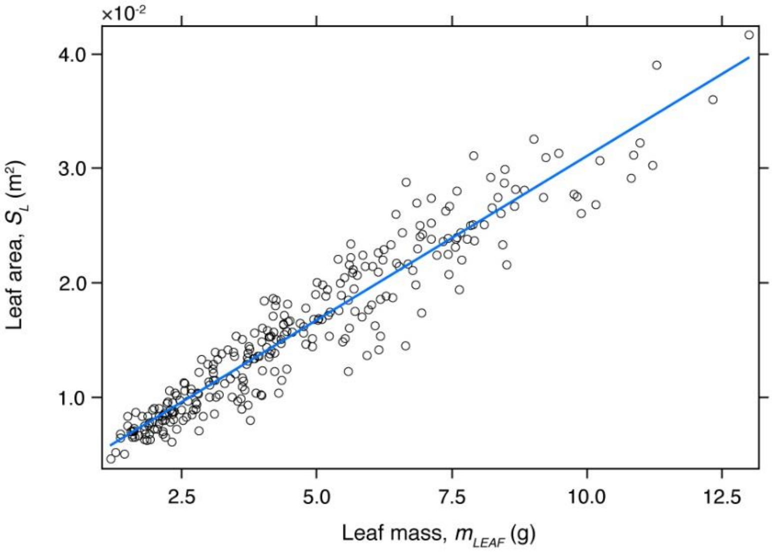

Figure 3: Scatter plot and best-fit line of single-sided leaf surface area, S_{LEAF} (m^2), against fresh leaf mass, m_{LEAF} (g), for 280 leaves sampled from three *Khaya senegalensis*. Least-squares regression equation is $S_{LEAF} = 2.87\times10^{-3}$ (m_{LEAF}) + 2.31×10^{-3} [$r^2 = 0.91$].

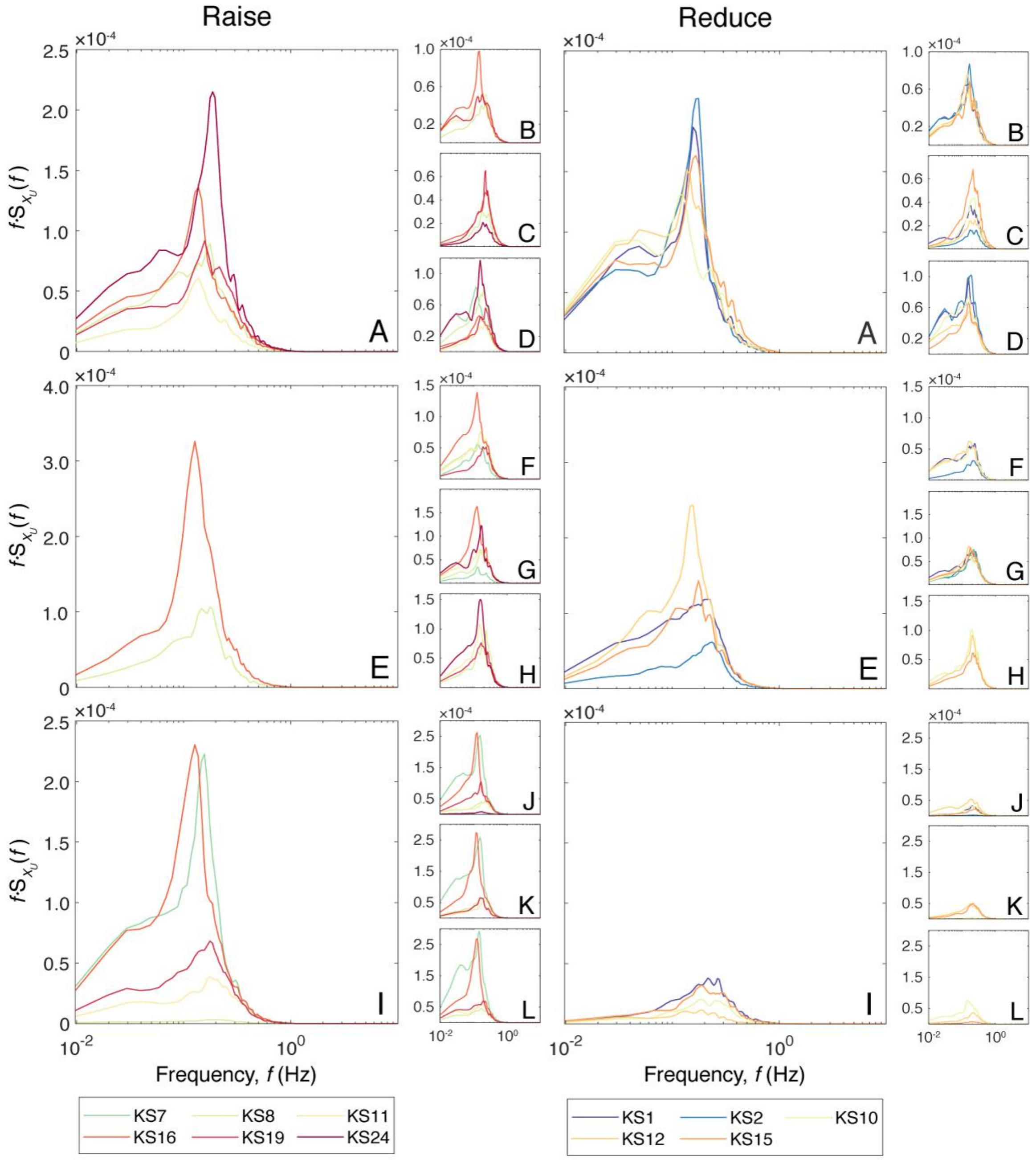

Figure 4: Fourier energy spectra $f{\cdot}S_{Xu}(f)$ computed using 30-minute time histories of streamwise trunk deformation, x_u, for raised (left columns) and reduced (right columns) *Khaya senegalensis*. At 0% (A – D), 10% (E – H), and 20% (I – L) pruning severity, each large image and three adjacent outset images shows Fourier spectra for 30-minute intervals with the highest average wind speeds. See Table 1 for 30-minute average wind speeds and prevailing directions measured during each 30-minute interval. In the legends, trees are identified by the abbreviation KS and tree number.

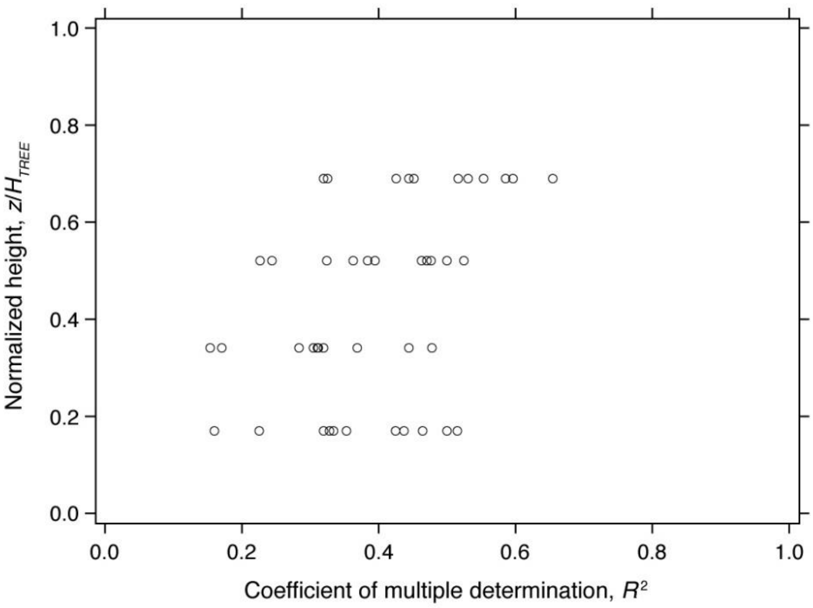

Figure 5: For all unpruned *Khaya senegalensis*, scatterplot of the coefficient of multiple determination (R^2) describing the proportion of variance in 30-minute maximum bending moment, M_B (kN·m), explained by 30-minute maximum wind speed, U (m·s^{-1}), using a quadratic function for wind speeds measured on four different anemometers installed 4.6, 9.1, 13.7, and 18.3 m above ground. The installation height of anemometers, z (m), was normalized by the average height of *K. senegalensis*, H_{TREE} = 26.9 m.

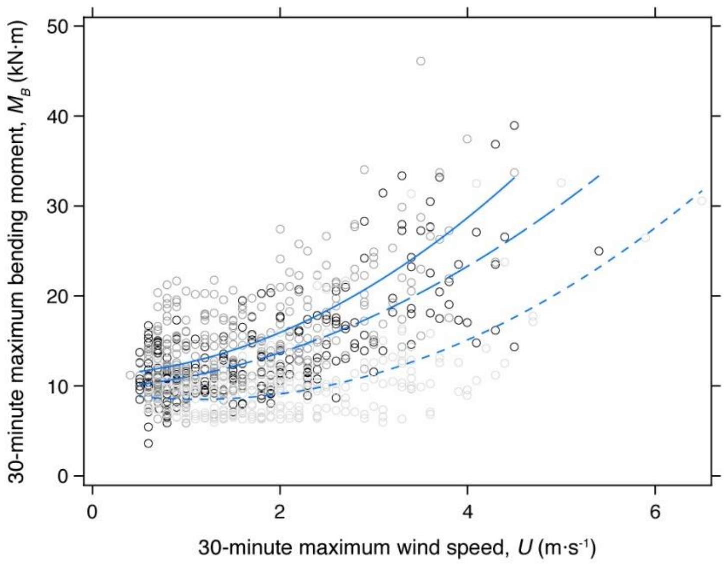

A

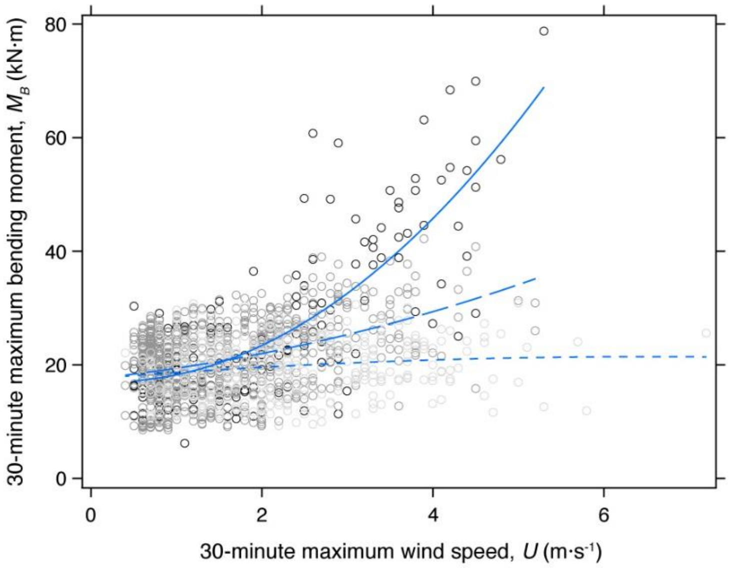

B

Figure 6: For raised (**A**) and reduced (**B**) *Khaya senegalensis*, scatter plot and best-fit lines of 30-minute maximum bending moment, M_B (kN·m), against 30-minute maximum wind speed, U (m·s^{-1}), measured 18.3 m above ground (z/H_{TREE} = 0.69) at 0% (black empty circle marker, solid line), 10% (dark gray empty circle marker, long dash line), and 20% (light gray empty circle marker, short dash line) pruning severity. For raised trees, least squares regression equations at 0%, 10%, and 20% severity are $M_B = 0.70\ U^2 + 0.61\ U + 9.67$ (n = 230; R^2 = 0.52), $M_B = 1.00\ U^2 + 0.38\ U + 11.2$ (n = 312; R^2 = 0.48), and $M_B = 0.81\ U^2 – 1.83\ U + 9.55$ (n = 278; R^2 = 0.38), respectively. For reduced trees, least squares regression equations at 0%, 10%, and 20% severity are $M_B = 2.02\ U^2 + 7.80\ U + 25.3$ (n = 288; R^2 = 0.56), $M_B = 0.43\ U^2 + 6.96\ U + 26.5$ (n = 825; R^2 = 0.41), and $M_B = -0.66\ U^2 + 4.49\ U + 27.3$ (n = 370; R^2 = 0.03), respectively.

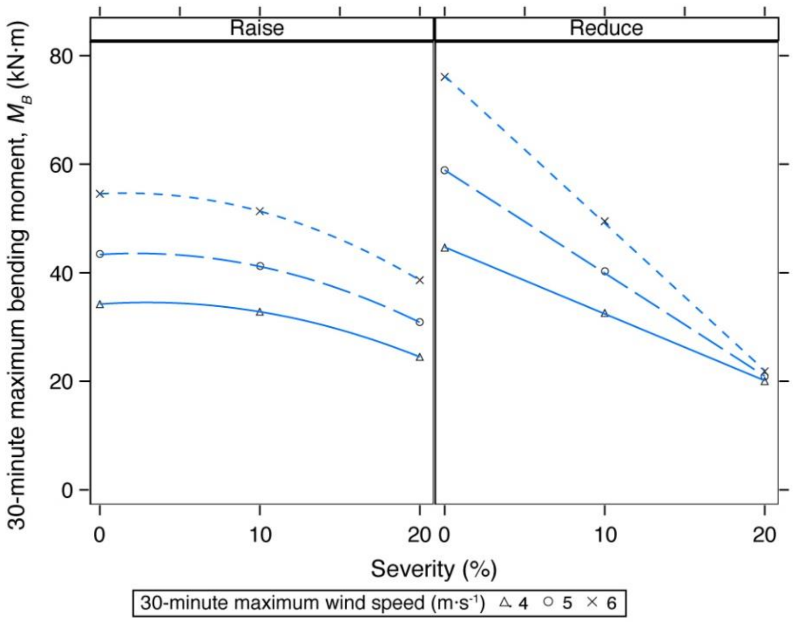

Figure 7: Regression of mean *Khaya senegalensis* 30-minute maximum bending moment, M_B (kN·m), against pruning severity for raised (left panel) and reduced (right panel) trees at three different values of the covariate 30-minute maximum wind speed, U (m·s^{-1}). During the experiment, wind-induced M_B was measured repeatedly on the lower trunk of six raised and five reduced *K. senegalensis*. For raised trees, least squares regression equations are $M_B = (-3.46\times10^{-2})\ U^2 + (2.06\times10^{-1})\ U + 34.2$ ($R^2 = 1$), $M_B = (-4.04\times10^{-2})\ U^2 + (1.83\times10^{-1})\ U + 43.4$ ($R^2 = 1$), and $M_B = (-4.75\times10^{-2})\ U^2 + (1.54\times10^{-1})\ U + 54.6$ ($R^2 = 1$) at 4, 5, and 6 m·s^{-1}, respectively. For reduced trees, least squares regression equations are $M_B = -1.23\ U + 44.7$ ($R^2 = 0.99$), $M_B = -1.90\ U + 58.9$ ($r^2 = 0.99$), and $M_B = -2.71\ U + 76.3$ ($r^2 = 0.99$) at 4, 5, and 6 m·s^{-1}, respectively.

Table 1: Wind conditions during 30-minute intervals used for spectral analysis

Pruning Severity	Start date and time	Average Wind speed ($m \cdot s^{-1}$)	Prevailing Wind Direction (°)	Standard Deviation of Wind Direction (°)
0%				
A	6 Sep 2013 23:19	1.2	100	28
B	7 Sep 2013 12:15	1.2	90	19
C	14 Sep 2013 13:30	1.0	315	39
D	15 Sep 2013 12:19	1.2	45	39
10%				
E	5 Oct 2013 05:01	1.6	135	13
F	11 Oct 2013 13:15	0.8	315	40
G	16 Oct 2013 15:30	1.0	315	36
H	20 Oct 2013 13:30	1.2	90	22
20%				
I	23 Dec 2013 15:19	1.8	180	18
J	7 Jan 2014 09:30	2.0	180	17
K	10 Jan 2014 14:20	1.9	180	15
L	10 Jan 2014 16:00	2.1	188	22

Note: The prevailing wind direction was determined as the mode of all observations, and the standard deviation of wind direction was estimated using the unbiased estimate (Yamartino, 1984). See Figure 4 for the corresponding Fourier spectra computed for each 30-minute interval.

Table 2: Model coefficients for covariate fit to 30-minute maximum M_B (kN·m) and 30-minute maximum U^2 ($m \cdot s^{-1}$)

Effect	Level	Parameter Estimate (95% CI)	*p*
U^2 × Type × Severity	Raise 0%	1.02 (0.90 – 1.13)	< 0.001
	Raise 10%	0.93 (0.82 – 1.03)	< 0.001
	Raise 20%	0.71 (0.63 – 0.79)	< 0.001
	Reduce 0%	1.57 (1.48 – 1.67)	< 0.001
	Reduce 10%	0.84 (0.77 – 0.92)	< 0.001
	Reduce 20%	0.09 (0.01 – 0.16)	0.025

Note: Parameter estimates for covariates describe the slope of a linear relationship between 30-minute maximum M_B and 30-minute maximum U^2 for all combinations of pruning type and severity. See Table 3 for the full model and tests of fixed effects.

Table 3: Analysis of covariance of 30-minute maximum bending moment, M_B (kN·m), measured on the lower trunk of *Khaya senegalensis*, after accounting for 30-minute maximum wind speed, U (m·s^{-1})

Effect	**df**	***F***	***p***	**Level**	**Mean (SE)**
Type	1, 9.4	0.07	0.796		
Severity	2, 6218	308	< 0.001		
Type × Severity	2, 6218	72.6	< 0.001		
U^2 × Type × Severity	6, 8539	407	< 0.001		
Severity:Type$_1$(Raise) at $U = 4$	2, 3207	56.0	< 0.001		
Orthogonal polynomial comparisons					
Linear	1, 614	79.3	< 0.001		
Quadratic	1, 963	14.3	< 0.001	0%	34.2 (3.8)
				10%	32.8 (3.8)
				20%	24.5 (3.8)
Severity:Type$_2$(Reduce) at $U = 4$	2, 2672	394	< 0.001		
Orthogonal polynomial comparisons					
Linear	1, 2124	680	< 0.001		
Quadratic	1, 3301	6.72	0.010	0%	44.6 (4.1)
				10%	32.6 (4.1)
				20%	20.0 (4.1)
Severity:Type$_1$(Raise) at $U = 5$	2, 6565	39.6	< 0.001		
Orthogonal polynomial comparisons					
Linear	1, 1831	64.3	< 0.001		
Quadratic	1, 2673	9.41	0.002	0%	43.4 (3.9)
				10%	41.2 (3.9)
				20%	30.9 (3.8)
Severity:Type$_2$(Reduce) at $U = 5$	2, 5715	395	< 0.001		
Orthogonal polynomial comparisons					
Linear	1, 4154	754	< 0.001		
Quadratic	1, 5710	3.38	0.066	0%	58.8 (4.2)
				10%	40.2 (4.2)
				20%	20.8 (4.1)
Severity:Type$_1$(Raise) at $U = 6$	2, 8175	29.7	< 0.001		
Orthogonal polynomial comparisons					
Linear	1, 3061	52.1	< 0.001		
Quadratic	1, 3591	6.70	0.010	0%	54.6 (4.2)
				10%	51.3 (4.1)
				20%	38.6 (3.9)
Severity:Type$_2$(Reduce) at $U = 6$	2, 7257	373	< 0.001		
Orthogonal polynomial comparisons					
Linear	1, 5212	753	< 0.001		
Quadratic	1, 6614	1.95	0.163	0%	76.1 (4.4)
				10%	49.5 (4.3)
				20%	21.8 (4.2)

Note: Fixed effects include pruning type: raise, reduce; severity: 0, 10, 20%; and their interaction: type × severity. Statistical inferences about fixed effects were made with the covariate equal to 5 m·s^{-1}. During the experiment, 30-minute maximum M_B was measured repeatedly on six raised and five reduced *K. senegalensis*. Orthogonal polynomial comparisons test the significance of an *n*th-order polynomial multiple regression of 30-minute maximum M_B against pruning severity after accounting for 30-minute maximum U; the corresponding regression coefficients were determined separately using least squares regression (Figure 7).

Online Resource 1

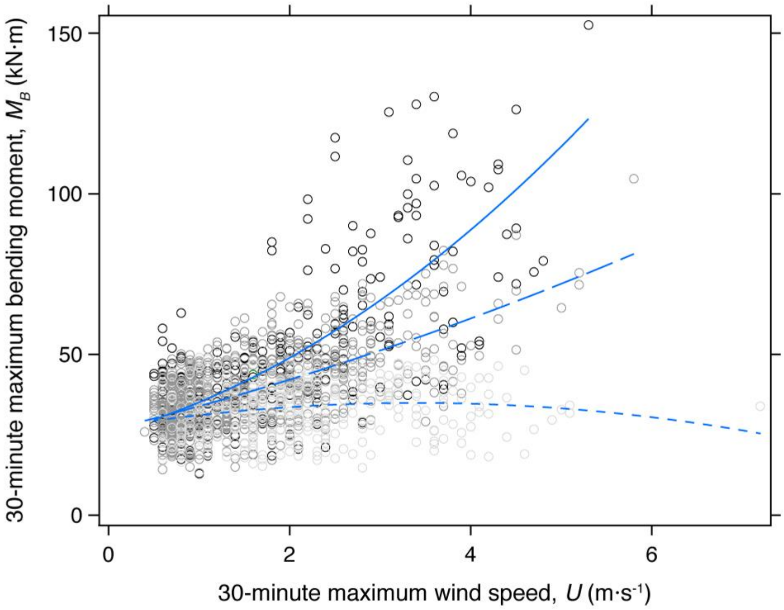

Figure OR1: Scatter plot and best-fit lines of the 30-minute maximum bending moment, M_B (kN·m), against 30-minute maximum wind speed, U (m·s^{-1}), measured 18.3 m above ground (z/H_{TREE} = 0.69) for *Khaya senegalensis* tree number 1 reduced by 0% (black empty circle marker, solid line), 10% (dark gray empty circle marker, long dash line), and 20% (light gray empty circle marker, short dash line). At 0%, 10%, and 20% severity, least squares regression equations are $M_B = 2.02\ U^2 + 7.80\ U + 25.3$ (n = 288; R^2 = 0.56), $M_B = 0.43\ U^2 + 6.96\ U + 26.5$ (n = 825; R^2 = 0.41), and $M_B = -0.66\ U^2 + 4.49\ U + 27.3$ (n = 370; R^2 = 0.03), respectively.

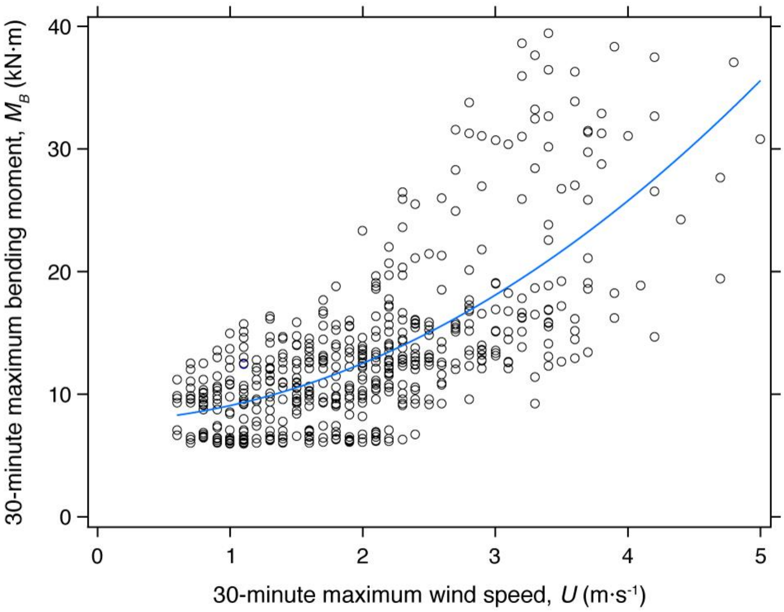

Figure OR2: Scatter plot and best-fit lines of the 30-minute maximum bending moment, M_B (kN·m), against 30-minute maximum wind speed, U (m·s^{-1}), measured 18.3 m above ground (z/H_{TREE} = 0.69) for *Khaya senegalensis* tree number 7 reduced by 20%. Due to instrumentation failures, no observations were available at 0% and 10% severity for this tree. Least squares regression equation is $M_B = 1.06\ U^2 + 0.26\ U + 7.75$ (n = 507; R^2 = 0.48).

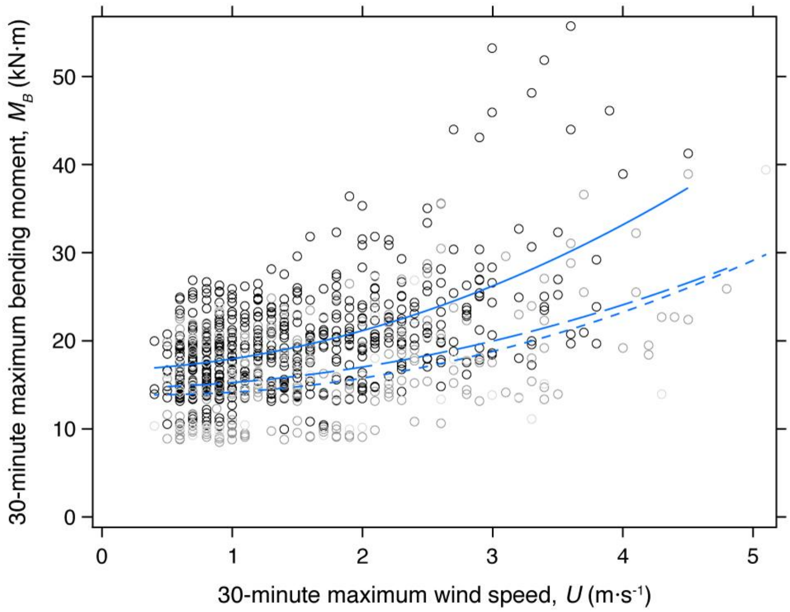

Figure OR3: Scatter plot and best-fit lines of the 30-minute maximum bending moment, M_B (kN·m), against 30-minute maximum wind speed, U (m·s^{-1}), measured 18.3 m above ground (z/H_{TREE} = 0.69) for *Khaya senegalensis* tree number 8 raised by 0% (black empty circle marker, solid line), 10% (dark gray empty circle marker, long dash line), and 20% (light gray empty circle marker, short dash line). At 0%, 10%, and 20% severity, least squares regression equations are $M_B = 0.94\ U^2 + 0.40\ U + 16.6$ ($n = 551$; $R^2 = 0.29$), $M_B = 0.59\ U^2 + 0.01\ U + 14.7$ ($n = 243$; $R^2 = 0.20$), and $M_B = 0.71\ U^2 - 0.53\ U + 14.0$ ($n = 48$; $R^2 = 0.26$), respectively.

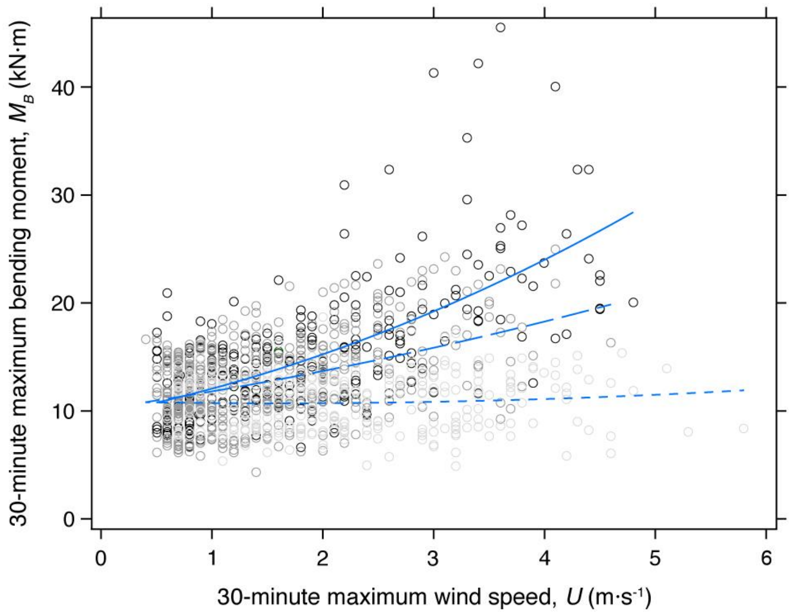

Figure OR4: Scatter plot and best-fit lines of the 30-minute maximum bending moment, M_B (kN·m), against 30-minute maximum wind speed, U (m·s^{-1}), measured 18.3 m above ground (z/H_{TREE} = 0.69) for *Khaya senegalensis* tree number 10 reduced by 0% (black empty circle marker, solid line), 10% (dark gray empty circle marker, long dash line), and 20% (light gray empty circle marker, short dash line). At 0%, 10%, and 20% severity, least squares regression equations are $M_B = 0.70\ U^2 + 0.61\ U + 9.67$ ($n = 230$; $R^2 = 0.52$), $M_B = 1.00\ U^2 + 0.38\ U + 11.2$ ($n = 312$; $R^2 = 0.48$), and $M_B = 0.81\ U^2 - 1.83\ U + 9.55$ ($n = 278$; $R^2 = 0.38$), respectively.

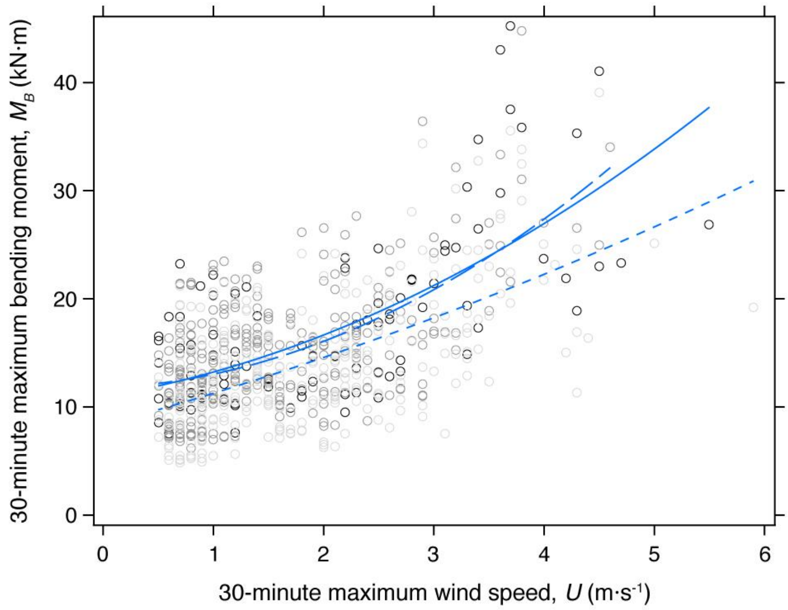

Figure OR5: Scatter plot and best-fit lines of the 30-minute maximum bending moment, M_B (kN·m), against 30-minute maximum wind speed, U (m·s^{-1}), measured 18.3 m above ground (z/H_{TREE} = 0.69) for *Khaya senegalensis* tree number 11 raised by 0% (black empty circle marker, solid line), 10% (dark gray empty circle marker, long dash line), and 20% (light gray empty circle marker, short dash line). At 0%, 10%, and 20% severity, least squares regression equations are $M_B = 0.58\ U^2 + 1.69\ U + 11.0$ (n = 109; R^2 = 0.48), $M_B = 0.87\ U^2 + 0.41\ U + 11.7$ (n = 288; R^2 = 0.36), and $M_B = 0.18\ U^2 + 2.78\ U + 8.31$ (n = 297; R^2 = 0.36), respectively.

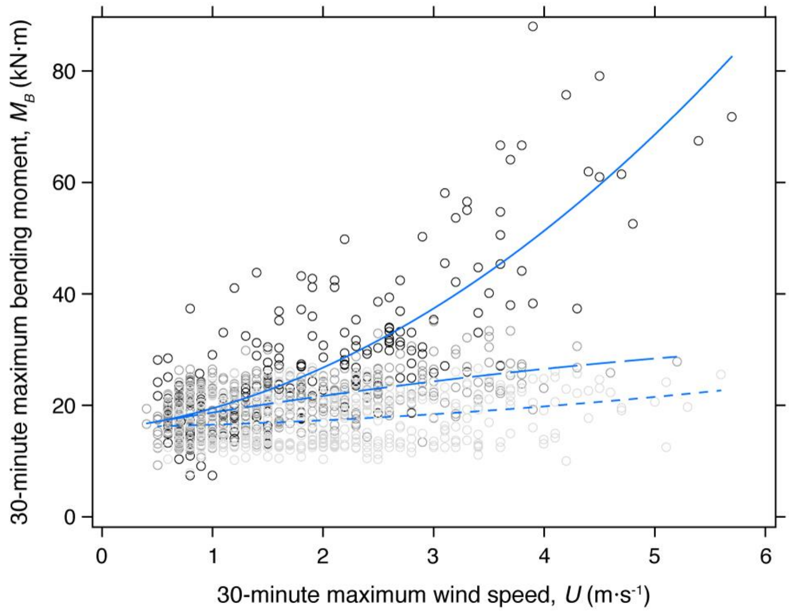

Figure OR6: Scatter plot and best-fit lines of the 30-minute maximum bending moment, M_B (kN·m), against 30-minute maximum wind speed, U (m·s^{-1}), measured 18.3 m above ground (z/H_{TREE} = 0.69) for *Khaya senegalensis* tree number 12 reduced by 0% (black empty circle marker, solid line), 10% (dark gray empty circle marker, long dash line), and 20% (light gray empty circle marker, short dash line). At 0%, 10%, and 20% severity, least squares regression equations are $M_B = 1.66\ U^2 + 2.32\ U + 15.5$ (n = 233; R^2 = 0.64), $M_B = -0.19\ U^2 + 3.54\ U + 15.4$ (n = 386; R^2 = 0.32), and $M_B = 0.15\ U^2 + 0.33\ U + 16.1$ (n = 441; R^2 = 0.06), respectively.

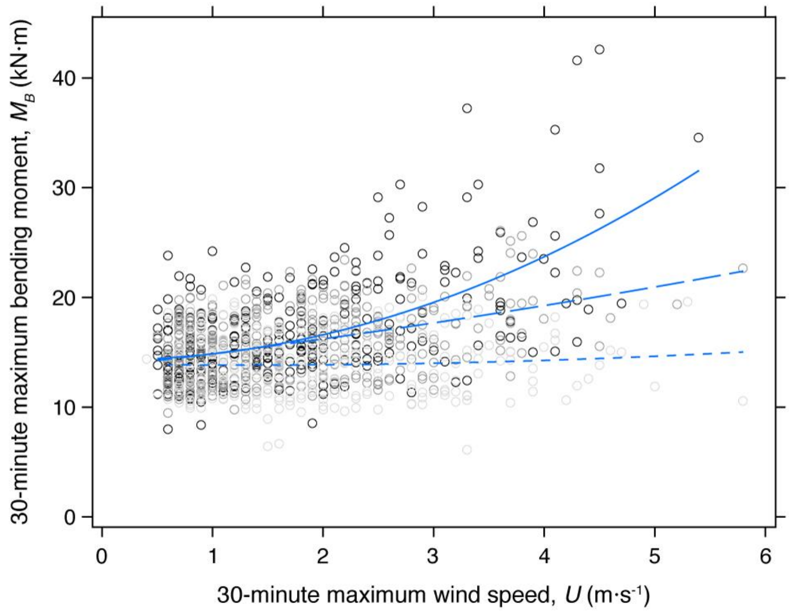

Figure OR7: Scatter plot and best-fit lines of the 30-minute maximum bending moment, M_B (kN·m), against 30-minute maximum wind speed, U (m·s^{-1}), measured 18.3 m above ground (z/H_{TREE} = 0.69) for *Khaya senegalensis* tree number 15 reduced by 0% (black empty circle marker, solid line), 10% (dark gray empty circle marker, long dash line), and 20% (light gray empty circle marker, short dash line). At 0%, 10%, and 20% severity, least squares regression equations are $M_B = 0.60\ U^2 - 0.07\ U + 14.3$ (n = 305; R^2 = 0.33), $M_B = 0.06\ U^2 + 1.17\ U + 13.6$ (n = 416; R^2 = 0.18), and $M_B = 0.06\ U^2 - 0.15\ U + 13.9$ (n = 250; R^2 = 0.00), respectively.

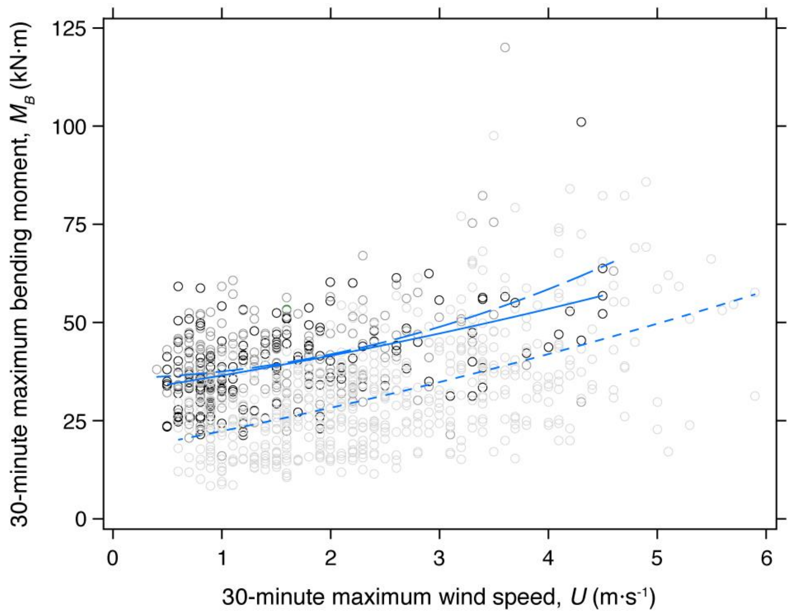

Figure OR8: Scatter plot and best-fit lines of the 30-minute maximum bending moment, M_B (kN·m), against 30-minute maximum wind speed, U (m·s^{-1}), measured 18.3 m above ground (z/H_{TREE} = 0.69) for *Khaya senegalensis* tree number 19 raised by 0% (black empty circle marker, solid line), 10% (dark gray empty circle marker, long dash line), and 20% (light gray empty circle marker, short dash line). At 0%, 10%, and 20% severity, least squares regression equations are $M_B = 0.31\ U^2 + 4.11\ U + 32.1$ (n = 175; R^2 = 0.26), $M_B = 1.31\ U^2 + 0.45\ U + 35.8$ (n = 213; R^2 = 0.17), and $M_B = 0.30\ U^2 + 5.03\ U + 17.0$ (n = 543; R^2 = 0.29), respectively.

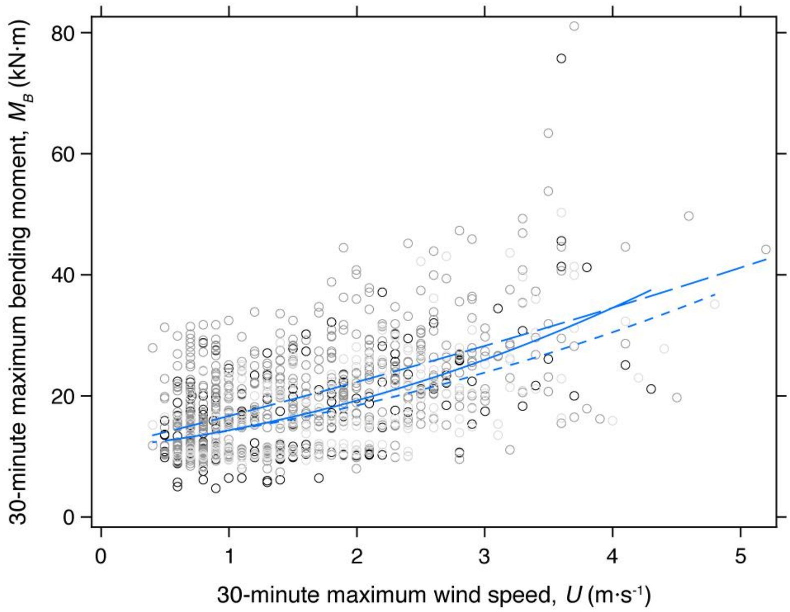

Figure OR9: Scatter plot and best-fit lines of the 30-minute maximum bending moment, M_B (kN·m), against 30-minute maximum wind speed, U (m·s^{-1}), measured 18.3 m above ground (z/H_{TREE} = 0.69) for *Khaya senegalensis* tree number 24 raised by 0% (black empty circle marker, solid line), 10% (dark gray empty circle marker, long dash line), and 20% (light gray empty circle marker, short dash line). At 0%, 10%, and 20% severity, least squares regression equations are $M_B = 0.92\ U^2 + 2.14\ U + 11.3$ (n = 177; R^2 = 0.34), $M_B = 0.17\ U^2 + 5.12\ U + 11.4$ (n = 620; R^2 = 0.31), and $M_B = 0.62\ U^2 + 2.32\ U + 11.3$ (n = 244; R^2 = 0.33), respectively.